Vietnam Journal of Mechanics, VAST, Vol. 36, No 4 (2014), pp. 267 – 281

# TRANSIENT ANALYSIS OF LAMINATED COMPOSITE PLATES USING NURBS-BASED ISOGEOMETRIC ANALYSIS

**Lieu B. Nguyen[1], Chien H. Thai[2], Ngon T. Dang[1], H. Nguyen-Xuan[3,*]**
[1] *Ho Chi Minh City University of Technology and Education, Vietnam*
[2] *Ton Duc Thang University, Ho Chi Minh City, Vietnam*
[3] *Vietnamese-German University, Ho Chi Minh City, Vietnam*
*E-mail: hung.nx@vgu.edu.vn
Received July 04, 2014

**Abstract.** We further study isogeometric approach for response analysis of laminated composite plates using the higher-order shear deformation theory. The present theory is derived from the classical plate theory (CPT) and the shear stress free surface conditions are naturally satisfied. Therefore, shear correction factors are not required. Galerkin weak form of response analysis model for laminated composite plates is used to obtain the discrete system of equations. It can be solved by isogeometric approach based on the non-uniform rational B-splines (NURBS) basic functions. Some numerical examples of the laminated composite plates under various dynamic loads, fiber orientations and lay-up numbers are provided. The accuracy and reliability of the proposed method is verified by comparing with analytical solutions, numerical solutions and results from Ansys software.

*Keywords.* Transient analysis, laminated composite plate, isogeometric analysis, NURBS, Newmark integration.

## 1. INTRODUCTION

The transient response of laminated composite plates has received much attention from designers due to increasing applications of composite in high performance aircraft, vehicles and vessels. Whether they are used in civil, marine or aerospace, most structures are subjected to dynamic loads during their operation. Therefore, there exists a need for assessing the natural frequency and transient response of structures.

Many numerical methods have been developed to compute, analyze and simulate the response as well as dynamic characteristics of laminated composite plates. Out of these methods, the finite element method (FEM) has become the universally applicable technique for solving boundary and initial value problems. In the past years, Reismann [1], Reismann and Lee [2] have analyzed simply supported rectangular isotropic plates, which are subjected to suddenly a uniformly distributed load over a square area on the plate. The transient finite element analysis of isotropic plate was also carried out by

Rock and Hinton [3] for thick and thin plates. Akay [4] determined the large deflection transient response of isotropic plates using a mixed FEM. For composite plates, Reddy [5] presented finite element results for the transient analysis of layered composite plates based on the first-order shear deformation theory (FSDT). Mallikarjuna and Kant [6] presented an isoparametric finite element formulation based on a higher-order displacement model for dynamic analysis of multi-layer symmetric composite plate. Wang and his co-workers developed the strip element method (SEM) for static bending analysis of orthotropic plates. Then, Wang et al. [7] extended the SEM to analyze dynamic response of symmetric laminated plates.

Although FEM is an extremely versatile and powerful technique, it has certain disadvantages. Recently, Hughes and his co-workers have proposed a robustly computational isogeometric analysis [8]. Following this approach, the CAD-shape functions, commonly the non-uniform rational B-splines (NURBS) are substituted for the Lagrange polynomial based shape functions in the CAE. The computational cost is decreased significantly as the meshes are generated within the CAD. IGA gives higher accurate results because of the smoothness and the higher-order continuity between elements [9, 10].

In this paper, a higher-order displacement field in which the in-plane displacement is expressed as cubic functions of the thickness coordinate with constant transverse displacement across the thickness is used. The finite element formulation based on the higher-order shear deformation theory (HSDT) requires elements with at least $C^1$-inter-element continuity. It is difficult to achieve such elements for free-form geometries when using the standard Lagrangian polynomials as basis functions. Fortunately, IGA can be easily obtained because NURBS basis functions are $C^{p-1}$ continuous. The governing equations of the laminated composite plates are transformed into a standard weak-form, which is then discretized into the system of time-dependent equations to be solved by the unconditionally stable Newmark time integration scheme. Several numerical examples with many different models are provided to illustrate the effectiveness and reliability of the present method in comparison with other results from the literature.

The paper is outlined as follows. Next section introduces the HSDT for laminated composite plates. In section 3, the numerical formulation relied on the HSDT and IGA is described. The numerical results and discussions are provided in section 4. Finally, in section 5, concluding remarks are presented with the brief discussion of the numerical results obtained by the developed methodology.

## 2. THE HIGHER-ORDER SHEAR DEFORMATION THEORY FOR PLATES

Let $\Omega$ be the domain in $\mathbb{R}^2$ occupied by the mid-plane of the plate and $u_0, v_0, w$ and $\beta = (\beta_x; \beta_y)^T$ denote the displacement components in the $x; y; z$ directions and the rotations in the $x-z$ and $y-z$ planes (or the-$y$ and the-$x$ axes), respectively. Fig. 1 shows the geometry of a plate and the coordinate system. A generalized displacement field of an arbitrary point in the plate based on higher-order shear deformation theory derived from the classical plate theory is defined as follows [9]

$$
\begin{aligned}
u(x,y,z,t) &= u_0(x,y,t) - z\frac{\partial w(x,y,t)}{\partial x} + f(z)\,\beta_x(x,y,t)\\
v(x,y,z,t) &= v_0(x,y,t) - z\frac{\partial w(x,y,t)}{\partial y} + f(z)\,\beta_y(x,y,t), \left(\frac{-h}{2} \le z \le \frac{h}{2}\right)\\
w(x,y,z,t) &= w(x,y,t)
\end{aligned}
\tag{1}
$$

In this paper we exploit the third-order shear deformation theory (TSDT) of Reddy [11] and the distribution function is written as $f(z) = z - 4z^3/3h^2$.

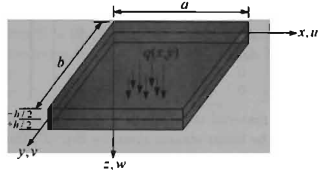


*Fig. 1.* Plate model and coordinate system

The relationship between strains and displacements is described by

$$
\begin{aligned}
\boldsymbol{\varepsilon_p} &= [\varepsilon_{xx}\ \varepsilon_{yy}\ \gamma_{xy}]^T = \boldsymbol{\varepsilon}_0 + z\boldsymbol{\varepsilon}_1 + f(z)\boldsymbol{\varepsilon}_2,\\
\boldsymbol{\gamma} &= [\gamma_{xz}\ \gamma_{yz}]^T = f'(z)\boldsymbol{\varepsilon}_s
\end{aligned}
\tag{2}
$$

where

$$
\boldsymbol{\varepsilon}_0 = \begin{bmatrix} \dfrac{\partial u_0}{\partial x} \\ \dfrac{\partial v_0}{\partial y} \\ \dfrac{\partial v_0}{\partial x} + \dfrac{\partial u_0}{\partial y} \end{bmatrix}, \boldsymbol{\varepsilon}_1 = \begin{bmatrix} -\dfrac{\partial^2 w}{\partial x^2} \\ -\dfrac{\partial^2 w}{\partial y^2} \\ -2\dfrac{\partial^2 w}{\partial x \partial y} \end{bmatrix}, \boldsymbol{\varepsilon}_2 = \begin{bmatrix} \dfrac{\partial \beta_x}{\partial x} \\ \dfrac{\partial \beta_y}{\partial y} \\ \dfrac{\partial \beta_y}{\partial x} + \dfrac{\partial \beta_x}{\partial y} \end{bmatrix}, \boldsymbol{\varepsilon}_s = \begin{bmatrix} \beta_x \\ \beta_y \end{bmatrix} \tag{3}
$$

Neglecting $\sigma_z$ for each orthotropic layer, the constitutive equation of an orthotropic lamina in the local coordinate system is derived from Hooke's law for a plane stress condition as

$$
\begin{Bmatrix} \sigma_1^k \\ \sigma_2^k \\ \tau_{12}^k \\ \tau_{13}^k \\ \tau_{23}^k \end{Bmatrix} = \begin{bmatrix} Q_{11} & Q_{12} & 0 & 0 & 0 \\ Q_{12} & Q_{22} & 0 & 0 & 0 \\ 0 & 0 & Q_{33} & 0 & 0 \\ 0 & 0 & 0 & Q_{55} & 0 \\ 0 & 0 & 0 & 0 & Q_{44} \end{bmatrix}^k \begin{Bmatrix} \varepsilon_1^k \\ \varepsilon_2^k \\ \gamma_{12}^k \\ \gamma_{13}^k \\ \gamma_{23}^k \end{Bmatrix}, \tag{4}
$$

where subscripts 1 and 2 are the directions of the fiber and in-plane normal to fiber, respectively, subscript 3 indicates the direction normal to the plate, and the reduced stiffness components, $Q_{ij}^k$ are given by

$$Q_{11}^k = \frac{E_1^k}{1-\nu_{12}^k\nu_{21}^k}, Q_{12}^k = \frac{\nu_{12}^k E_2^k}{1-\nu_{12}^k\nu_{21}^k}, Q_{22}^k = \frac{E_2^k}{1-\nu_{12}^k\nu_{21}^k}, Q_{33}^k = G_{12}^k, Q_{55}^k = G_{13}^k, Q_{44}^k = G_{23}^k, \tag{5}$$

in which $E_1, E_2, G_{12}, G_{23}, G_{13}$ and $\nu_{12}$ are independent material properties for each layer.

The laminate is usually made of several orthotropic layers. Each layer must be transformed into the laminate coordinate system $(x, y, z)$. The stress-strain relationship is given as

$$\begin{Bmatrix} \sigma_{xx}^k \\ \sigma_{yy}^k \\ \tau_{xy}^k \\ \tau_{xz}^k \\ \tau_{yz}^k \end{Bmatrix} = \begin{bmatrix} \bar{Q}_{11} & \bar{Q}_{12} & \bar{Q}_{16} & 0 & 0 \\ \bar{Q}_{12} & \bar{Q}_{22} & \bar{Q}_{26} & 0 & 0 \\ \bar{Q}_{61} & \bar{Q}_{62} & \bar{Q}_{33} & 0 & 0 \\ 0 & 0 & 0 & \bar{Q}_{55} & \bar{Q}_{54} \\ 0 & 0 & 0 & \bar{Q}_{45} & \bar{Q}_{44} \end{bmatrix}^k \begin{Bmatrix} \varepsilon_{xx}^k \\ \varepsilon_{yy}^k \\ \gamma_{xy}^k \\ \gamma_{xz}^k \\ \gamma_{yz}^k \end{Bmatrix}, \tag{6}$$

where $\bar{Q}_{ij}^k$ is the transformed material constant matrix (see [12] for more details).

From Hooke's law and the linear strains given by Eq. (2), the stress is computed by

$$\boldsymbol{\sigma} = \begin{Bmatrix} \boldsymbol{\sigma}_p \\ \boldsymbol{\tau} \end{Bmatrix} = \begin{bmatrix} \mathbf{D}^s & 0 \\ 0 & \mathbf{D}^s \end{bmatrix} \begin{Bmatrix} \boldsymbol{\varepsilon}_p \\ \boldsymbol{\gamma} \end{Bmatrix}, \tag{7}$$

where $\boldsymbol{\sigma}_p$ and $\boldsymbol{\tau}$ are the in-plane stress component and shear stress, respectively, and $\mathbf{D}^s$ is material constant matrices given in the form as

$$\mathbf{D}^s = \begin{bmatrix} \mathbf{A} & \mathbf{B} & \mathbf{E} \\ \mathbf{B} & \mathbf{D} & \mathbf{F} \\ \mathbf{E} & \mathbf{F} & \mathbf{H} \end{bmatrix}, \tag{8}$$

where

$$\begin{aligned} &A_{ij}, B_{ij}, D_{ij}, E_{ij}, F_{ij}, H_{ij} = \int_{-h/2}^{h/2} (1, z, z^2, f(z), zf(z), f^2(z))\bar{Q}_{ij}dz, \quad i,j = 1,2,6, \\ &D_{ij}^s = \int_{-h/2}^{h/2} \left[(f'(z))^2\right] \bar{Q}_{ij}dz, \quad i,j = 4,5. \end{aligned} \tag{9}$$

For forced vibration analysis of the plates, a weak form can be derived from the following undamped dynamic equilibrium equation as

$$\int_\Omega \delta\boldsymbol{\varepsilon}_p^T \mathbf{D}^s \boldsymbol{\varepsilon}_p d\Omega + \int_\Omega \delta\boldsymbol{\gamma}^T \mathbf{D}^s \boldsymbol{\gamma} d\Omega + \int_\Omega \delta\bar{\mathbf{u}}^T \mathbf{m}\ddot{\bar{\mathbf{u}}} d\Omega = \int_\Omega \delta w q(x,y,t) d\Omega, \tag{10}$$

where $q(x, y, t)$ is the transverse loading per unit area and the function depending on time and space; the mass matrix $\mathbf{m}$ is calculated according to the consistent form given by

$$\mathbf{m} = \begin{bmatrix} I_1 & I_2 & I_4 \\ I_2 & I_3 & I_5 \\ I_4 & I_5 & I_6 \end{bmatrix}, (I_1, I_2, I_3, I_4, I_5, I_6) = \int_{-h/2}^{h/2} \rho\left(1, z, z^2, f(z), zf(z), f^2(z)\right)dz, \tag{11}$$

in which $\bar{\mathbf{u}} = \begin{bmatrix} \mathbf{u}_1 & \mathbf{u}_2 & \mathbf{u}_3 \end{bmatrix}^T$ with

$$\mathbf{u}_1 = \begin{Bmatrix} u_0 \\ v_0 \\ w \end{Bmatrix}, \quad \mathbf{u}_2 = \begin{Bmatrix} -w_{,x} \\ -w_{,y} \\ 0 \end{Bmatrix}, \quad \mathbf{u}_3 = \begin{Bmatrix} \beta_x \\ \beta_y \\ 0 \end{Bmatrix}, \tag{12}$$

where $\rho$ is the mass density.

## 3. THE LAMINATED COMPOSITE PLATE FORMULATION BASED ON NURBS BASIS FUNCTIONS

### 3.1. Introduction to NURBS basis functions [9]

Given a knot vector $\Xi = \{\xi_1, \xi_2, \ldots, \xi_{n+p+1}\}$, the associated B-spline basis functions are defined recursively starting with the zero$^{th}$ order basis function ($p = 0$) as

$$N_{i,0}(\xi) = \begin{Bmatrix} 1 & \text{if} \quad \xi_i \le \xi < \xi_{i+1} \\ 0 & \text{otherwise} \end{Bmatrix}, \tag{13}$$

and for a polynomial order $p \ge 1$

$$N_{i,p}(\xi) = \frac{\xi - \xi_i}{\xi_{i+p} - \xi_i} N_{i,p-1}(\xi) + \frac{\xi_{i+p+1} - \xi}{\xi_{i+p+1} - \xi_{i+1}} N_{i+1,p-1}(\xi). \tag{14}$$

A knot vector $\Xi$ is defined as a sequence of knot value $\xi_i \in \mathbb{R}, i = 1, \ldots, n+p$. If the first and the last knots are repeated $p+1$ times, the knot vector is called open knot.

By the tensor product of basis functions in two parametric dimensions $\xi$ and $\eta$ with two knot vectors $\Xi = \{\xi_1, \xi_2, \ldots, \xi_{n+p+1}\}$ and $\mathrm{H} = \{\eta_1, \eta_2, \ldots, \eta_{m+q+1}\}$, the two-dimensional B-spline basis functions are obtained as, $N_A(\xi, \eta) = N_{i,p}(\xi) M_{j,q}(\eta)$. Fig. 2 illustrates a bivariate cubic B-spline basic function.

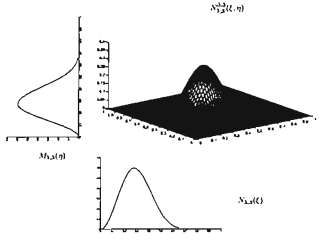

*Fig. 2.* A bivariate cubic B-spline basis function with knot vectors $\Xi = \mathrm{H} = \{0, 0, 0, 0, 0.25, 0.5, 0.75, 1, 1, 1, 1\}$

To exactly represent some curved geometries (e.g. circles, cylinders, spheres, etc.) the non-uniform rational B-splines (NURBS) functions are used. Being different from B-spline, each control point of NURBS has additional value called an individual weight $\zeta_A$ [8]. Thus, the NURBS functions can be expressed as $R_A(\xi,\eta) = N_A\zeta_A / \sum_{A=1}^{m\times n} N_A(\xi,\eta)\zeta_A$. It is clear that B-spline function is only the special case of the NURBS function when the individual weight of control point is constant.

### 3.2. A higher-order plate formulation based on NURBS approximation

Using the NURBS basis functions defined above, both the description of the geometry (or the physical point) and the displacement field $\mathbf{u}$ of the plate are approximated as

$$\mathbf{x}^h(\xi,\eta) = \sum_{A=1}^{m\times n} R_A(\xi,\eta)\mathbf{P}_A; \quad \mathbf{u}^h(\xi,\eta) = \sum_{A=1}^{m\times n} R_A(\xi,\eta)\mathbf{q}_A, \tag{15}$$

where $n \times m$ is the number basis functions, $\mathbf{x}^T = (x\ y)$ is the physical coordinate vector.

In Eq. (15), $R_A(\xi,\eta)$ is rational basic functions, $\mathbf{P}_A$ is the control points and $\mathbf{q}_A = \left[\begin{array}{ccccc} u_{0A} & v_{0A} & w_A & \beta_{xA} & \beta_{yA} \end{array}\right]^T$ is the vector of nodal degrees of freedom associated with the control point A.

Substituting Eq. (15) into Eq. (3), the in-plane and shear strains can be rewritten as

$$\left[\varepsilon_p\ \gamma\right]^T = \sum_{A=1}^{m\times n} \left[\begin{array}{ccccc} \mathbf{B}_A^m & \mathbf{B}_A^{b1} & \mathbf{B}_A^{b2} & \mathbf{B}_A^s \end{array}\right]^T \mathbf{q}_A, \tag{16}$$

in which

$$\begin{aligned} \mathbf{B}_A^m &= \left[\begin{array}{ccccc} R_{A,x} & 0 & 0 & 0 & 0 \\ 0 & R_{A,y} & 0 & 0 & 0 \\ R_{A,y} & R_{A,x} & 0 & 0 & 0 \end{array}\right], \quad \mathbf{B}_A^{b1} = \left[\begin{array}{ccccc} 0 & 0 & -R_{A,xx} & 0 & 0 \\ 0 & 0 & -R_{A,yy} & 0 & 0 \\ 0 & 0 & -2R_{A,xy} & 0 & 0 \end{array}\right] \\ \mathbf{B}_A^{b2} &= \left[\begin{array}{ccccc} 0 & 0 & 0 & R_{A,x} & 0 \\ 0 & 0 & 0 & 0 & R_{A,y} \\ 0 & 0 & 0 & R_{A,y} & R_{A,x} \end{array}\right], \quad \mathbf{B}_A^s = \left[\begin{array}{ccccc} 0 & 0 & 0 & R_A & 0 \\ 0 & 0 & 0 & 0 & R_A \end{array}\right]. \end{aligned} \tag{17}$$

For forced vibration analysis of the plates, undamped dynamic discrete equation can be written from Eq. (10) as

$$\mathbf{M}\ddot{\mathbf{q}} + \mathbf{K}\mathbf{q} = \mathbf{F}(t), \tag{18}$$

where the global stiffness matrix $\mathbf{K}$ is given by

$$\mathbf{K} = \int_\Omega \left[ \left\{\begin{array}{c} \mathbf{B}^m \\ \mathbf{B}^{b1} \\ \mathbf{B}^{b2} \end{array}\right\}^t \left[\begin{array}{ccc} \mathbf{A} & \mathbf{B} & \mathbf{E} \\ \mathbf{B} & \mathbf{D} & \mathbf{F} \\ \mathbf{E} & \mathbf{F} & \mathbf{H} \end{array}\right] \left\{\begin{array}{c} \mathbf{B}^m \\ \mathbf{B}^{b1} \\ \mathbf{B}^{b2} \end{array}\right\} + (\mathbf{B}^s)^T\mathbf{D}^s\mathbf{B}^s \right] d\Omega. \tag{19}$$

The distributed transverse force in the $z$ direction one has the following expression

$$\mathbf{F}(t) = \int_\Omega \mathbf{R}q(x,y,t)d\Omega, \tag{20}$$

where

$$\mathbf{R} = \begin{bmatrix} 0 & 0 & R_A & 0 & 0 \end{bmatrix}. \tag{21}$$

The global mass matrix $\mathbf{M}$ is given as

$$\mathbf{M} = \int_{\Omega} \left\{ \begin{bmatrix} \mathbf{N}_1 \\ \mathbf{N}_2 \\ \mathbf{N}_3 \end{bmatrix}^T \begin{bmatrix} I_1 & I_2 & I_4 \\ I_2 & I_3 & I_5 \\ I_4 & I_5 & I_6 \end{bmatrix} \begin{bmatrix} \mathbf{N}_1 \\ \mathbf{N}_2 \\ \mathbf{N}_3 \end{bmatrix} \right\} d\Omega, \tag{22}$$

where

$$\mathbf{N}_1 = \begin{bmatrix} R_A & 0 & 0 & 0 & 0 \\ 0 & R_A & 0 & 0 & 0 \\ 0 & 0 & R_A & 0 & 0 \end{bmatrix}; \mathbf{N}_2 = \begin{bmatrix} 0 & 0 & -R_{A,x} & 0 & 0 \\ 0 & 0 & -R_{A,y} & 0 & 0 \\ 0 & 0 & 0 & 0 & 0 \end{bmatrix}; \mathbf{N}_3 = \begin{bmatrix} 0 & 0 & 0 & R_A & 0 \\ 0 & 0 & 0 & 0 & R_A \\ 0 & 0 & 0 & 0 & 0 \end{bmatrix}. \tag{23}$$

It should be noted that for forced vibration analysis, the approximate function is done with both space and time. For the displacements and accelerations at time $t + \Delta t$, Eq. (18) should be considered at time $t + \Delta t$ as follows

$$\mathbf{M}\ddot{\mathbf{q}}_{t+\Delta t} + \mathbf{K}\mathbf{q}_{t+\Delta t} = \mathbf{F}_{t+\Delta t}(t). \tag{24}$$

To solve this second order time dependent problem, several methods have been proposed such as, Wilson, Newmark, Houbolt, Crank-Nicholson, etc. In this paper, Eq. (18) is solved by the Newmark time integration method. The Newmark method is an implicit method. This method assumes that the acceleration varies linearly within the interval $(t,\ t + \Delta t)$. The formulation of the Newmark method is [13]

$$[\mathbf{M} + \alpha\mathbf{K}(\Delta t)^2]\,\ddot{\mathbf{q}}_1 = \mathbf{F}_1 - [\mathbf{K}\mathbf{q}_0 + \mathbf{K}\Delta t\dot{\mathbf{q}}_0 + (\frac{1}{2} - \alpha)\mathbf{K}\ddot{\mathbf{q}}_0(\Delta t)^2], \tag{25}$$

$$\dot{\mathbf{q}}_1 = \dot{\mathbf{q}}_0 + (1 - \delta)\ddot{\mathbf{q}}_0\Delta t + \delta\ddot{\mathbf{q}}_1\Delta t, \tag{26}$$

$$\mathbf{q}_1 = \mathbf{q}_0 + \dot{\mathbf{q}}_0\Delta t + (\frac{1}{2} - \alpha)\ddot{\mathbf{q}}_0(\Delta t)^2 + \alpha\ddot{\mathbf{q}}_1(\Delta t)^2. \tag{27}$$

The parameters $\alpha$ and $\delta$ are constants whose values depend on the finite difference scheme used in the calculations. Two well-known and commonly used cases are average acceleration method ($\alpha = 1/4$ and $\delta = 1/2$) and linear acceleration method ($\alpha = 1/6$ and $\delta = 1/2$). Here we used the average acceleration method, which is unconditionally stable if $\delta \geq 0.5$ and $\alpha \geq 1/4(\delta + 0.5)^2$.

## 4. NUMERICAL EXAMPLES

### 4.1. A study of the convergence

Free vibration analysis of the laminated composite plates is investigated corresponding to right hand side of Eq. (18) equal to zero. Let us consider a four-layer $\{0^0/90^0/90^0/0^0\}$ square plate with simply supported boundary condition. The effects of the length to thickness $a/h$ and elastic modulus ratios $E_1/E_2$ are studied. To show the convergence of the present approach, the length to thickness $a/h = 5$ and elastic modulus ratios $E_1/E_2 = 40$ are used. As shown in Tab. 1, the normalized frequencies are computed using meshes of

$9 \times 9$, $13 \times 13$ and $17 \times 17$. It can be observed that the differences of normalized frequencies between meshes of $9 \times 9$ and $13 \times 13$ are not significant and between meshes of $13 \times 13$ and $17 \times 17$ are identical. Hence, for a comparison with other methods, a mesh of $13 \times 13$ cubic elements can be chosen. The first normalized frequency derived from the present approach is listed in Tab. 2 corresponding to various modulus ratios and $a/h = 5$. The obtained results are compared with analytical solutions based on the HSDT [14, 15] the moving least squares differential quadrature method (DQM) [16] based on the FSDT, the meshfree method using multiquadric radial basis functions (RBFs) [17] and wavelets functions [18] based on the FSDT. A good agreement is found for the present method in comparison with other ones. It is also seen that the present results match very well with the exact solutions [14, 15]. The influence of the length to thickness ratios is also considered as displayed in Tab. 3. The obtained results are compared with those of Zhen and Wanji [19] based on a global-local higher-order theory (GLHOT), Matsunaga [20] based on a global-local higher-order theory. Again, a good agreement with other published solutions is obtained.

*Table 1.* The convergence of non-dimensional frequency parameter $\varpi = \left(\omega a^2/h\right)\left(\rho/E_2\right)^{1/2}$ of a four layer $[0^0/90^0/90^0/0^0]$ simply supported laminated square plate $(a/h = 5)$

| Method | Meshes | | |
|---|---|---|---|
| | $9 \times 9$ | $13 \times 13$ | $17 \times 17$ |
| IGA (present) | 10.7876 | 10.7873 | 10.7873 |

*Table 2.* A non-dimensional frequency parameter $\varpi = \left(\omega a^2/h\right)\left(\rho/E_2\right)^{1/2}$ of a $[0^0/90^0/90^0/0^0]$ simply supported laminated square plate $(a/h = 5)$

| Method | $E_1/E_2$ | | | |
|---|---|---|---|---|
| | 10 | 20 | 30 | 40 |
| RBFs-FSDT [17] | 8.2526 | 9.4974 | 10.2308 | 10.7329 |
| Wavelets-FSDT [18] | 8.2794 | 9.5375 | 10.2889 | 10.8117 |
| DQM-FSDT [16] | 8.2924 | 9.5613 | 10.3200 | 10.8490 |
| Exact-HSDT [14, 15] | 8.2982 | 9.5671 | 10.3260 | 10.8540 |
| IGA (present) | 8.2718 | 9.5263 | 10.2719 | 10.7873 |

*Table 3.* A non-dimensional frequency parameter $\varpi = \left(\omega a^2/h\right)\left(\rho/E_2\right)^{1/2}$ of a $[0^0/90^0/90^0/0^0]$ simply supported laminated square plate $(E_1/E_2 = 40)$

| Methods | $a/h$ | | | | | | |
|---|---|---|---|---|---|---|---|
| | 4 | 5 | 10 | 20 | 25 | 50 | 100 |
| Zhen et al. [19] | 9.2406 | 10.7294 | 15.1658 | 17.8035 | 18.2404 | 18.9022 | 19.1566 |
| Matsunaga [20] | 9.1988 | 10.6876 | 15.0721 | 17.6369 | 18.0557 | 18.6702 | 18.8352 |
| IGA (present) | 9.3235 | 10.7873 | 15.1073 | 17.6466 | 18.0620 | 18.6718 | 18.8356 |

### 4.2. Transient analysis

In order to demonstrate the accuracy and effectiveness of the present method for transient analysis of laminated composite plates, four numerical examples with different transient loadings are studied. The obtained results are compared with other numerical or analytical solutions available in the literature or commercial software. For first three examples, cubic order NURBS basis function with 13×13 elements is used. All layers of the laminated plates are assumed to have the same thicknesses and material properties. The time step $\Delta t = 0.1$ ms is chosen for Sections 4.2.1 and 4.2.2.

**4.2.1.** *A three-layer square plate* $[0^0/90^0/0^0]$

First, a fully simply supported three-layer square laminated plate sorted as $[0^0/90^0/0^0]$ is considered. Material I is used, shown in Tab. 4. This example was also studied by Wang et al. [7] using the trip element method (SEM), which is chosen here to demonstrate the accuracy of the IGA in dynamic analysis of plates under different transient loads including step, triangular, sine and explosive blast loads. The length and the thickness of square plate are assumed to be $a = 20h$ and $h = 0.0381$ m, respectively. The plate is subjected to a transverse load which is sinusoidally distributed in spatial domain and varies with time as

$$q(x, y, t) = q_0 \sin(\frac{\pi x}{a}) \sin(\frac{\pi y}{b}) F(t), \tag{28}$$

in which

$$F(t) = \begin{cases} \left\{ \begin{array}{ll} 1 & 0 \le t \le t_1 \\ 0 & t > t_1 \end{array} \right\} & \text{Step loading} \\ \left\{ \begin{array}{ll} 1 - t/t_1 & 0 \le t \le t_1 \\ 0 & t > t_1 \end{array} \right\} & \text{Triangular loading} \\ \left\{ \begin{array}{ll} \sin(\pi t/t_1) & 0 \le t \le t_1 \\ 0 & t > t_1 \end{array} \right\} & \text{Sine loading} \\ e^{-\gamma t} & \text{Explosive blast loading} \end{cases} \tag{29}$$

where $t_1 = 0.006$ s, $\gamma = 330$ s$^{-1}$ and $q_0 = 3.448$ MPa.

*Table 4.* Properties of material

| Material | $E_1$(GPa) | $E_2$ (GPa) | $G_{12}$ (GPa) | $G_{13}$ (GPa) | $G_{23}$ (GPa) | $\nu_{12}$ | $\rho$ (kg/m$^3$) |
|---|---|---|---|---|---|---|---|
| I | 172.369 | 6.895 | 3.448 | 3.448 | 3.448 | 0.25 | 1603.03 |
| II | 172.369 | 6.895 | 3.448 | 3.448 | 1.379 | 0.25 | 1603.03 |
| III | 131.69 | 8.55 | 6.67 | 6.67 | 6.67 | 0.3 | 1610 |

Fig. 3 shows the time histories of central deflection of the plate under various dynamic loadings. The obtained results of present solution using IGA are compared with those obtained by Wang et al. [7] using the strip element method (SEM). As expected, the effectiveness of this work is fully believable when profiles relatively coincide with Wang et al.'s solutions.

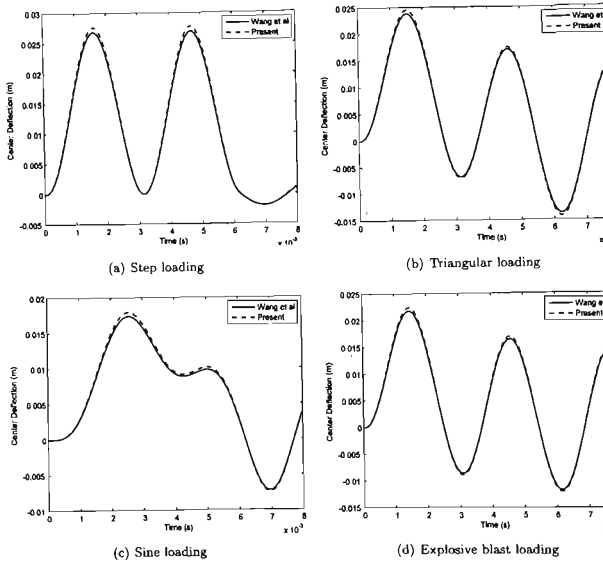


(a) Step loading

(b) Triangular loading

(c) Sine loading

(d) Explosive blast loading

*Fig. 3.* Variation of the center deflection as a function of time for a $(0^0/90^0/0^0)$ square laminated composite plate subjected to various dynamic loadings

Second, a fully simply supported three-layer square laminated plate sorted as $[0^0/90^0/0^0]$ is also considered. Material II is used. The length and thickness of the plates are assumed to be $a = 5h$ and $h = 0.1524$ m, respectively. As above example, the plate is also subjected to sinusoidally distributed transverse load (with $q_0 = 68.9476$ MPa). The displacement at the center of plate is also studied. Khdeir and Reddy [21] originally investigated this benchmark solution. Fig. 4 shows variation of the displacement at the center of plate as a function under various dynamic loadings. The present solutions based on IGA and TSDT are compared with exact solution of Khdeir and Reddy [21] using HSDT. As observed in Fig. 4, the profiles are relatively accurate, the error estimate is very small and approvable when comparing with exact solution.

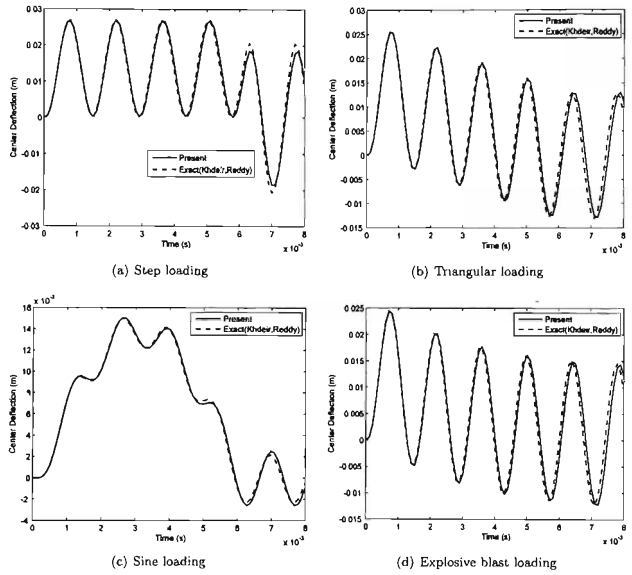


*Fig. 4.* Central deflection versus time for a $[0^0/90^0/0^0]$ square laminated plate subjected to various dynamic loadings

### 4.2.2. *A four-layer square plate* $[30^0/-30^0/-30^0/30^0]$

A fully clamped four-layer angle-ply square laminated plate with symmetrically stacking sequences $[30^0/-30^0/-30^0/30^0]$ is considered. Material III is used. The length to thickness ratio of the plate is assumed to be $a/h = 50$. The plate is also subjected to a transverse load which is uniformly distributed over the plate and is called conventional blast loading [7].

$$q(x, y, t) = q_0(1 - \frac{t}{t_2})e^{-\alpha_1 t/t_2}, \tag{30}$$

in which $q_0 = 68.9476$ KPa, $t_2 = 0.004$ s, $\alpha_1 = 1.98$.

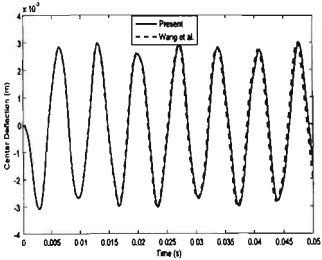


*Fig. 5.* The time history of the center deflection of the $[30^0/-30^0/-30^0/30^0]$ fully clamped laminated plate

The time history of the deflection at the center of the four-layer fully clamped (CCCC) laminated plate is investigated, as shown in Fig. 5. The results are compared with the solutions of Wang et al. [7]. From Fig. 5, the present results match well with the reference solutions.

**4.2.3.** *A circular four-layer plate* $[45^0/-45^0/-45^0/45^0]$

Finally, to increase lively for numerical examples and obtain the desired effect, we consider a $[45^0/-45^0/-45^0/45^0]$ circular plate with fully clamped (CCCC) boundary condition as shown Fig. 6a. Material parameter III is used. The plate is also subjected to a conventional blast load as given in Section 4.2.2. The circular plate has the radius to thickness ratio is 10 ($R/h = 10$). A rational quadratic basis is enough to model exactly the circular geometry. Coarse mesh and control net of the plate with respect to quadratic and cubic elements are illustrated in Fig. 7. Time step for transient analysis is chosen $\Delta t = 0.4$ ms. The plate is meshed with $13 \times 13$ NURBS cubic elements as shown Fig. 6b. Fig. 8 illustrates the profile of displacements versus time at the center of the circular plate


*Fig. 6.* The circular plate. (a) geometry and (b) mesh based on $13 \times 13$ cubic elements

subjected to conventional blast load. Obtained results are compared with solutions from ANSYS 13 which using SHELL 181 elements. It can be seen that the present solutions are in good agreement with the solutions from ANSYS software.

(a) $p = 2$ (b) $p = 3$

*Fig. 7.* Coarse mesh and control points of a circular plate with various degrees

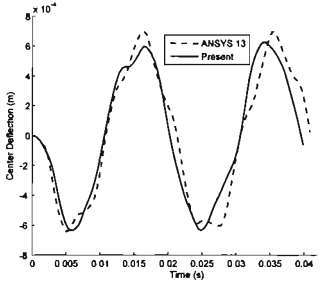


*Fig. 8.* The deflection at the center of the $[45^0/-45^0/-45^0/45^0]$ circular laminated plate subjected to a conventional blast load

## 5. CONCLUSIONS

Isogeometric analysis combined with TSDT to analyze the transient of laminated composite plates is first studied. The displacement field is generally defined and is derived from CPT. The Newmark time-integration algorithm was chosen to approximate the ordinary differential equations in time. We have successfully extended an application of the NURBS-based isogeometric finite element approach to analyze dynamic response for laminated composite plates as this work. IGA is the effectively numerical method. It has expressed well its role in solving the problems with just few elements especially curved

geometry as circle. The calculation of these problems has been done very fast. It not only helps to save costs but also increases the accuracy of solutions. The numerical results agreed well with those of available references and exact solution, and hence illustrated the accuracy and effectiveness of the present method.

## ACKNOWLEDGMENT

This research is funded by Vietnam National Foundation for Science and Technology Development (NAFOSTED) under grant number 107.02-2012.17. The support is gratefully acknowledged.

## REFERENCES

[1] H. Reismann. Forced motion of elastic plates. *Journal of Applied Mechanics*, **35**, (3), (1968), pp. 510–515.

[2] H. Reismann and Y. C. Lee. Forced motion of rectangular plates. *Developments in Theoretical and Applied Mechanics*, **4**, (1968), pp. 3–18.

[3] T. Rock and E. Hinton. Free vibration and transient response of thick and thin plates using the finite element method. *Earthquake Engineering & Structural Dynamics*, **3**, (1), (1974), pp 51–63.

[4] H. U. Akay. Dynamic large deflection analysis of plates using mixed finite elements. *Computers & Structures*, **11**, (1), (1980), pp. 1–11.

[5] J. N. Reddy. Dynamic (transient) analysis of layered anisotropic composite-material plates. *International Journal for Numerical Methods in Engineering*, **19**, (2), (1983), pp. 237–255.

[6] Mallikarjuna and T. Kant. Dynamics of laminated composite plates with a higher order theory and finite element discretization. *Journal of Sound and Vibration*, **126**, (3), (1988), pp. 463–475.

[7] Y. Wang, K. Lam, and G. Liu. A strip element method for the transient analysis of symmetric laminated plates. *International Journal of Solids and Structures*, **38**, (2), (2001), pp. 241–259.

[8] T. J. R. Hughes, J. A. Cottrell, and Y. Bazilevs. Isogeometric analysis: Cad, finite elements, NURBS, exact geometry and mesh refinement. *Computer Methods in Applied Mechanics and Engineering*, **194**, (39), (2005), pp. 4135–4195.

[9] C. H. Thai, A. J. M. Ferreira, S. P. A. Bordas, T. Rabczuk, and H. Nguyen-Xuan. Isogeometric analysis of laminated composite and sandwich plates using a new inverse trigonometric shear deformation theory. *European Journal of Mechanics-A/Solids*, **43**, (2014), pp. 89–108.

[10] N. Valizadeh, S. S. Ghorashi, H. Yousefi, T. Q. Bui, and T. Rabczuk. Transient analysis of laminated composite plates using isogeometric analysis. In *Proceedings of the Eighth International Conference on Engineering Computational Technology*, Civil-Comp Press, Stirlingshire, Scotland, (2012).

[11] J. N. Reddy. A simple higher-order theory for laminated composite plates. *Journal of Applied Mechanics*, **51**, (4), (1984), pp. 745–752.

[12] J N. Reddy. *Mechanics of laminated composite plates and shells: Theory and analysis*. CRC press, (2004).

[13] N. M. Newmark. A method of computation for structural dynamics. *Journal of the Engineering Mechanics Division*, **85**. (3), (1959), pp. 67–94

[14] A. A. Khdeir and L. Librescu. Analysis of symmetric cross-ply laminated elastic plates using a higher-order theory: Part II-buckling and free vibration. *Composite Structures*, **9**, (4), (1988), pp. 259–277.

[15] J. N. Reddy. *Mechanics of laminated composite plates: Theory and analysis*. CRC press Boca Raton, (1997).

[16] K. M. Liew, Y. Q. Huang, and J. N. Reddy. Vibration analysis of symmetrically laminated plates based on FSDT using the moving least squares differential quadrature method. *Computer Methods in Applied Mechanics and Engineering*, **192**, (19), (2003), pp. 2203–2222.

[17] A. J. M Ferreira. A formulation of the multiquadric radial basis function method for the analysis of laminated composite plates. *Composite Structures*, **59**, (3), (2003), pp. 385–392.

[18] A J. M. Ferreira, L Castro, and S. Bertoluzza. A high order collocation method for the static and vibration analysis of composite plates using a first-order theory. *Composite Structures*, **89**, (3), (2009), pp. 424–432.

[19] W. Zhen and C. Wanji. Free vibration of laminated composite and sandwich plates using global-local higher-order theory. *Journal of Sound and Vibration*, **298**, (1), (2006), pp. 333–349.

[20] H. Matsunaga. Vibration and stability of cross-ply laminated composite plates according to a global higher-order plate theory. *Composite Structures*, **48**, (4), (2000), pp. 231–244.

[21] A. A. Khdeir and J. N. Reddy. Exact solutions for the transient response of symmetric cross-ply laminates using a higher-order plate theory. *Composites Science and Technology*, **34**, (3), (1989), pp. 205–224.